ELSEVIER

Polymer 40 (1999) 2769–2777

polymer

The development of organized structures in polyethylene crystallized from a sheared melt, analyzed by WAXS and TEM

J.A. Pople[a], G.R. Mitchell[a,*], S.J. Sutton[a], A.S. Vaughan[a], C.K. Chai[b]

[a]*JJ Thomson Laboratory, University of Reading, Whiteknights, Reading, RG6 6AF, UK*
[b]*BP Chemicals s.n.c. Centre de Recherches, Bite Postale #6, Lavera, 13117, France*

Received 28 August 1997; revised 6 January 1998; accepted 3 March 1998

Abstract

The development of global orientation and morphological features in linear polyethylene crystallizing from a sheared melt are studied using in-situ time-resolving wide angle X-ray scattering (WAXS) and ex-situ transmission electron microscopy. It is found that samples subjected to a shear rate above a critical value of $\sim 1\ s^{-1}$ result in macroscopically oriented structures in the crystallized sample. This critical shear rate appears to be independent of the differences in molecular weight distribution of the samples studied although the morphologies which develop are sensitive to quite small differences in molecular weight distributions. The presence of shish kebabs in the morphology is shown to differ markedly according to variations in the upper molecular weight fraction of the molecular weight distribution, even though the resulting global orientation does not. The WAXS also reveals that areas which evidence no row nucleated structures still realize high degrees of molecular orientation. It is proposed that the formation of shish kebab or lamellar morphologies in these samples is dependent on the critical density of contiguous elongated crystallization nuclei rather than any specific global criteria.

Keywords: Polyethylene; Shear; Morphology

1. Introduction

Flow fields introduce a degree of anisotropy into polymer melts, which give rise to modified nucleation and crystallization behaviour. Often, this results in the formation of row nucleated structures, whose linear cores are concomitant with the axis of applied strain, as shown in the pioneering work of Keller and others on extensional flow [1–4]. Secondary crystallization then takes the form of epitaxial nucleation on the surface of the core structures, producing chain folded lamellae characteristically oriented, to a first approximation, perpendicular to the extension axis [4]. Later work [5,6], demonstrated that shish kebab structures also developed during crystallization from melts which had been subjected to prior shear flow. This work is concerned with the study of crystallization from such previously sheared melts and the relationship of the observed behaviour to models of crystallization developed for extensional flow.

Shish kebab morphologies result from the extension of the highest molecular weight fraction, even if this represents only a few percent of the overall distribution [7,8]. In fact, Janeschitz-Kriegl and coworkers have shown that the dependence of the rheological properties of molten linear polymers on the high molecular weight tail of the molecular weight distribution is critical to the extent that gel permeation chromatograms are insufficient for the prediction of the rheological characteristics of the polymer without mathematical extrapolation of the high tail of the curve [9–11].

Whilst the development of oriented crystal structures is often almost singularly associated with shish kebab structures, other morphological forms can also develop. Recently an overall kinetic equation incorporating the effect of shear rate was proposed by Monasse et al. [12,13]. This predicts the crystallization temperature and oriented layer thickness formed in polyethylene (PE) during an injection moulding procedure, by accounting for the different crystallization growth rates of the three orthogonal directions in a parallel plate shearing apparatus attached to a polarizing microscope [12]. They also demonstrated that the effect of shearing on the subsequent crystallization of an ethylene–propylene block copolymer is to enhance the number of nucleation sites for the formation of spherulitic structures: no row nucleated structures were seen in the resulting crystallized samples, which were melt sheared at shear rates up to $\dot{\gamma} = 2\ s^{-1}$ [13].

It is clear from these and other studies that a range of morphological forms, ranging from shish kebabs to spherulites, can develop from sheared melts. In this study, the morphological variability was studied in detail by applying

* Corresponding author.

0032-3861/99/$ - see front matter
PII: S0032-3861(98)00202-X

Table 1
Compositional data for the grades of polyethylene used in this work. M_n refers to the number average, M_w corresponds to the weight average molecular weight, both obtained by GPC. τ_{250} is obtained through dynamic viscosity measurements and corresponds to the time for the relaxation modulus required to reach 250 Pa

Polyethylene	M_w	M_n	M_w/M_n	τ_{250}
A	345 000	36 000	9.6	920
B	133 600	16 100	8.3	22
C	325 000	19 600	16.6	120

complementary in-situ X-ray scattering and electron microscopy techniques to samples of linear polyethylene with different but technologically typical molecular weight distributions. Molten PE was subjected to shear flow, and the orientational characteristics of the structural features which arose upon subsequent crystallization from the sheared melt were studied. We employed wide angle X-ray scattering (WAXS) as a method by which the global degree of orientation of polymer chain segments could be quantified, and dynamic measurements were taken in situ in a rheometer with controlled shear rate and temperature, in order to monitor the development of the crystalline state directly.

Previously, we have shown that the shearing of molten PE leads to small degrees of global orientation, ($\langle P_2 \rangle \sim 0.01$) in the melt [14]. By crystallizing the sheared PE in situ at 120°C it was shown that orientation parameters an order of magnitude higher were obtained if the prior melt shear rate exceeded a critical value: $\dot{\gamma}_c \sim 1\ s^{-1}$. The X-ray diffraction pattern of the crystallized PE evidenced four maxima around the scattering from the (110) crystal planes, though the precise morphology of the sample remained unknown. Nevertheless, it was proposed that this increased orientation in the crystalline state related to linear nuclei arising from the shear induced extension of the longest molecules.

The purpose of this work is twofold; to reveal the role of the molecular weight distribution in determining the orientation which develops under shear flow conditions and to examine the relationship between molecular orientation and morphology in samples crystallized from the sheared melt. In this respect we have employed in-situ WAXS measurements and ex-situ transmission electron microscopy (TEM) to explore local variations in the structure of the samples, (for which the X-ray diffraction provides only a global scenario), in order to extend the current understanding of the molecular scale behaviour associated with the crystallization of a sheared PE melt.

2. Experimental

2.1. Materials

The three samples employed here are linear grades of PE supplied by BP Chemicals and are typical of commercial

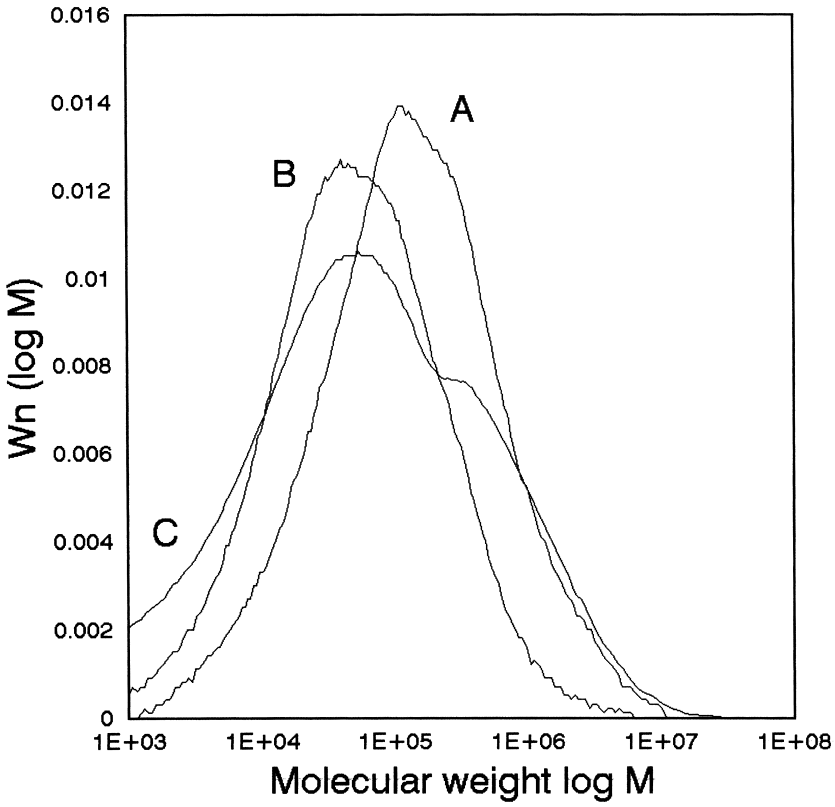

Fig. 1. GPC curves recorded for the linear grades of PE used in this work.

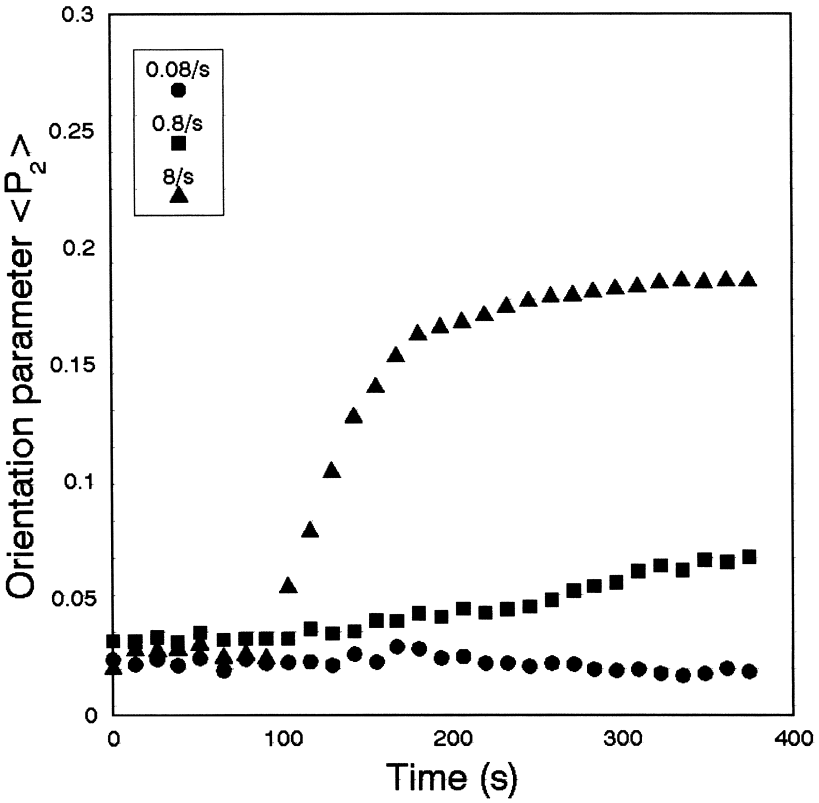

Fig. 2. Global orientation parameters $\langle P_2 \rangle$ as a function of time during the crystallization of PE sample A at 120°C which has been subject to a prior shear rate of 8 s^{-1} in the melt at 140°C. The time $t = 0$ s corresponds to the time at which the shearing ceased and the cooling simultaneously began.

materials. These materials differ with respect to their molecular weight distributions and average molecular weight data are detailed in Table 1.

In view of the central role of the molecular weight distribution in this work, we also show the GPC curves in Fig. 1. From this, it is clear that, although all these materials span a similar weight range, a number of detailed differences do exist. Sample C contains a bimodal molecular weight distribution with a pronounced second peak situated at $\sim 10^5$ which is absent in both A and B. Samples B and C both peak at similar molecular weights, whereas the maximum in the distribution for A occurs at a rather higher value. Finally above 10^6, A and C appear to contain comparable high molecular fractions whereas B includes fewer long molecules. However, since GPC is an unreliable means of probing the ultra high molecular weight fractions, dynamic viscosity measurements were also made. Polymeric materials exhibit a spectrum of relaxation times, the characteristics of which are related to the molecular weight distribution [15]. We have measured the storage and loss moduli for each PE sample at a temperature of 250°C and fitted the data using a series of Maxwell-type relaxation modes using the IRIS software package; each mode has an associated strength and relaxation time. A polymer relaxation time, τ_{250} was defined as the time over which the strength of the relaxation modulus had fallen to a reference value of 250 Pa. These polymer relaxation times were used to estimate the fraction of high molecular weight material present in each polymer. The data presented show that the highest level of high molecular weight fraction is present in sample A, whilst the lowest level is present in sample B.

2.2. Rheometer

The rheometer in which the samples are melted and sheared is a modified parallel plate cell produced by Linkam, and has been described previously [16]. The sample is contained between two steel plates, each of which is in close thermal contact with a silver block heater. Apertures in the plates allow transmission of the X-ray beam and are covered with 25 μm thick Kapton windows. The gap between the plates is controlled by four micrometer screws, and was set at ~ 100 μm for these experiments. The shear rate of the rheometer is controlled from a remote, programmable controller, and can be continuously varied to give shear rates between $\dot{\gamma} = 0.01$ s^{-1} and 100 s^{-1}. Visually patterned samples were used to test and confirm that wall slippage did not take place in the shear rate range considered in this work.

2.3. X-ray scattering

We used the Daresbury Synchrotron Radiation source for the time-resolving measurements and a laboratory based sealed 1.6 kW X-ray tube with a copper anode for the steady

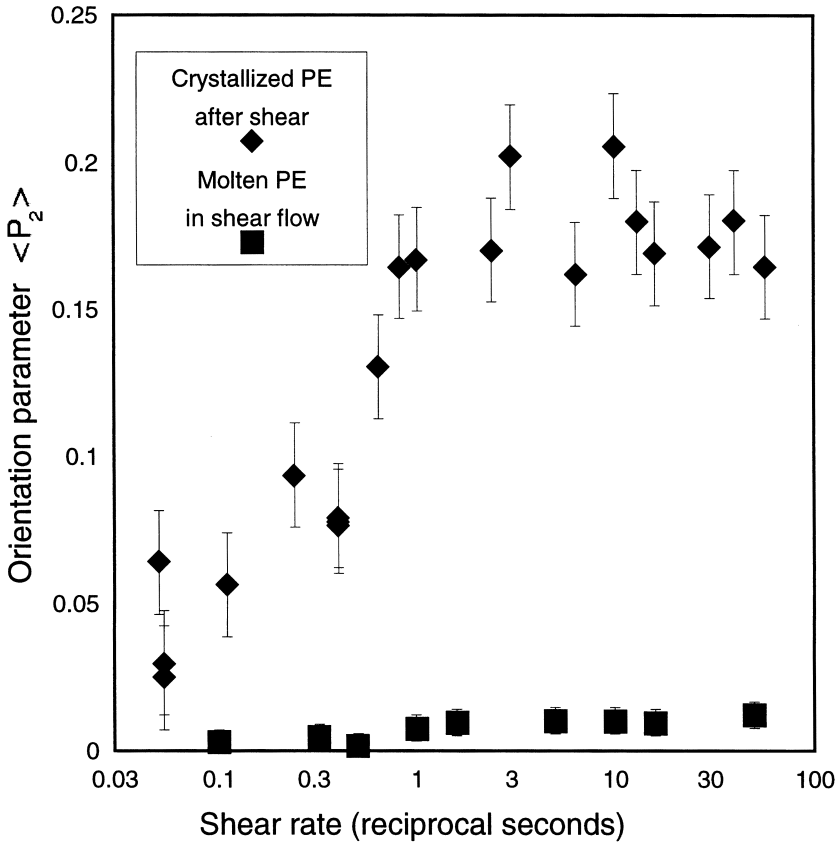

Fig. 3. Global orientation parameters $\langle P_2 \rangle$ as a function of the applied rate of shear for polyethylene A: sheared in the melt at 140°C (■), and subsequently rapidly crystallized (▲). In the crystalline systems, no distinction is made between the crystalline and non-crystalline scattering when determining the orientation parameter.

state measurements. The X-ray scattering data are collected using the Area X-ray Imaging System (AXIS) developed at The University of Reading [17,18]. Values of the orientation parameters, $\langle P_{2n}(\cos \alpha) \rangle$, of the PE chain segments in the melt and crystal planes in the solid-state are derived from the azimuthal distribution of intensities $I(\alpha)$ at a constant scattering vector within the X-ray diffraction patterns using methods described previously [14,19,20]. The probe beam provides scattering from an area which is large in relation to the structural units of the polymer, and therefore the information revealed from the diffraction data is in the form of global averages. The value of the azimuthal angle $\alpha = 0$ is assigned to the vertical direction, which is also the direction of shear.

2.4. Morphology

In contrast to X-ray scattering, TEM provides spatially resolved morphological information, with a resolution which is ideal for examining the lamellar detail within semi-crystalline polymers. Permanganic etching, which has proven to be a most useful technique for revealing the morphology of a whole range of polymers, was performed on the samples according to standard procedures, for a period of 4 h [21–23]. This allows a sufficient amount of material to be removed from the surface of the samples to eliminate any surface specific morphologies. Two stage replicas were then taken from areas equivalent to those from which X-ray data were collected (i.e. at the same radial distance from the centre of the sample). All the replicas were shadowed radially and TEM was performed using a Philips EM301 operating at 80 kV.

3. Results

3.1. Global molecular orientation from WAXS patterns

Discs of PE were melted in the shear cell and held at a constant temperature of 140°C. Each sample was subjected to one shear rate from a series of increasing shear rates, and the in-situ X-ray scattering data were used to derive the orientation parameter $\langle P_2 \rangle$. After shearing at a fixed shear rate for 8 min, the shear flow was stopped and simultaneously the samples were cooled to 120°C: the cooling took approximately 60 s. The in-situ X-ray scattering data permitted the ensuing crystallization process to be monitored. A typical result showing the developing anisotropy during crystallization of material A is displayed in Fig. 2. This level of anisotropy is calculated from the (110) crystal

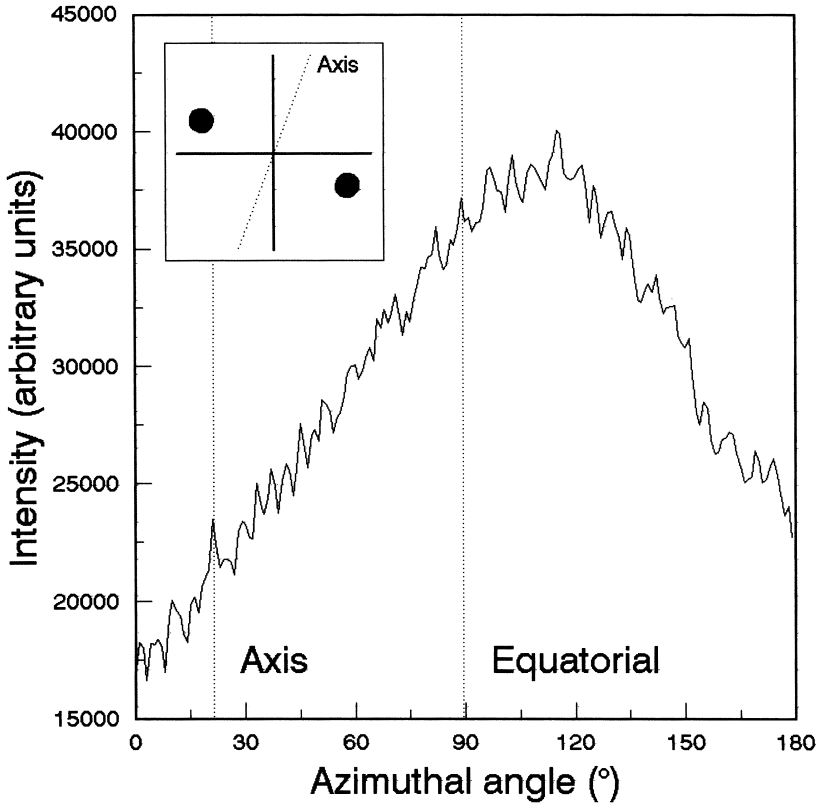

Fig. 4. Semi-azimuthal profile of the (110) crystal plane extracted from a WAXS pattern taken from PE sample A, crystallized at 120°C from a melt at 140°C sheared at 40 s^{-1}. A zero azimuthual angle corresponds to the meridional axis which is parallel to the flow axis. The equatorial axis at 90° is parallel to the vorticity vector. The inset schematic indicates the general nature of the X-ray diffraction pattern; the dots marking the position of the diffraction maxima. In the inset the flow axis is vertical. The symmetry axis of the diffraction pattern is shown on the profile and in the inset by means of a broken line and marked 'Axis'.

planes: no other reflections, such as (200) and (020), were available as the limited diameter of the exit aperture of the rheometer restricted the maximum recordable diffraction angle.

The final level of anisotropy, which was reached for each different prior shear rate, is plotted in Fig. 3. It can be seen that the high plateau level of orientation of crystalline PE is only obtained for shear rates greater than a critical value of $\dot{\gamma}_c \sim 1\ s^{-1}$. Similar results are obtained for samples B and C and reveal the novel result that although the plateau level of crystalline orientation differs from sample to sample, the critical shear rate, $\dot{\gamma}_c$, does not. Nevertheless, we suggest that this does not imply that $\dot{\gamma}_c$ is independent of the molecular weight distribution, since such an assertion is not physically reasonable. Rather, the apparent invariance of $\dot{\gamma}_c$ is a simple consequence of the materials considered in which the molecular weight distributions overlap to a considerable extent as shown in Fig. 1 and the apparent invariance of $\dot{\gamma}_c$ reflects the similarity of materials A, B and C in the mid to upper range of molecular weight. This observation is particularly important in view of the dramatic effects described below. It should be borne in mind when comparing the detail of the orientation parameters for the three samples, that each sample has been subjected to the same shear history in terms of shear strain. However, since each sample has a different molecular weight distribution, clearly the resultant variation in viscosity will lead to different shear histories in terms of shear stress.

Fig. 4 shows the WAXS data obtained from material A, after melt shearing and crystallization. This is presented in the form of a scattered intensity as a function of the azimuthal angle (zero when parallel to the flow axis) together with, inset, a schematic representation of the WAXS pattern. For the inset, the axis of the applied shear flow is vertical and the horizontal line is parallel to the vorticity vector. In this material, the scattering pattern takes the form of a two point pattern which, as shown schematically, is offset from the shear axis by $\sim 20°$. The symmetry axis for the diffraction pattern is shown in the inset and in the intensity versus angle plot as a dotted line and marked 'axis'. Since the intensity data are only presented over the azimuthal range 0–180° (the range 180–360° being symmetry related), this two point diffraction pattern manifests itself as a single broad maximum at 105°. The skewed nature of the diffraction pattern can be seen from the displacement of the peak maximum at 105° from the equatorial position at 90°. Figs. 5 and 6 show the equivalent results obtained for samples B and C. In these two samples, the X-ray patterns exhibit four azimuthal maxima, with the symmetry axis, (now at the saddle

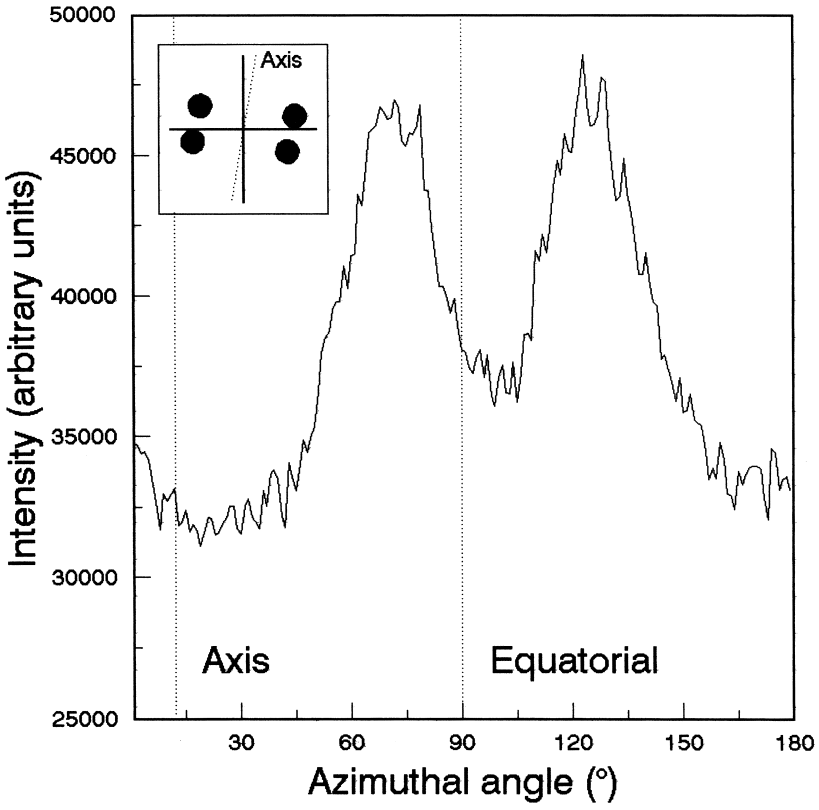

Fig. 5. Semi-azimuthal profile of the (110) crystal plane extracted from a WAXS pattern taken from PE sample B, crystallized at 120°C from a melt at 140°C sheared at 40 s^{-1}. See caption for Fig. 4.

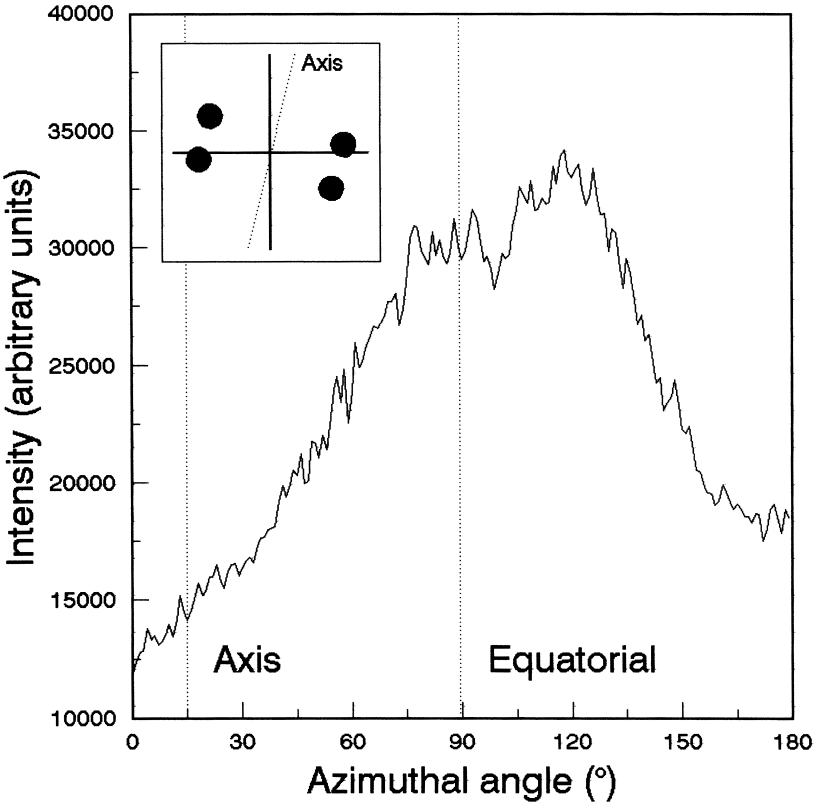

Fig. 6. Semi-azimuthal profile of the (110) crystal plane extracted from a WAXS pattern taken from PE sample C, crystallized at 120°C from a melt at 140°C sheared at 40 s^{-1}. See caption for Fig. 4.

Table 2
Measures of the crystalline component of the global molecular orientation parameter $\langle P_2 \rangle_x$, and the percentage of crystalline scattering at that scattering vector. Degrees of uncertainty are calculated from the statistical distribution of results obtained from each of the four quadrants

Polyethylene	Crystalline scattering	$\langle P_2 \rangle_x$ from (110)
A	0.65 ± 0.02	0.33 ± 0.02
B	0.66 ± 0.02	0.57 ± 0.02
C	0.64 ± 0.02	0.41 ± 0.02

between the two pairs of maxima), tilted at $\sim 20°$, as before. Thus the semi-azimuthal profiles for samples B and C display two maxima. The skewed symmetry axis is common for all samples, and is attributed to the radial nature of the deformation axis in simple shear.

The crystalline component of the WAXS patterns can be separated from the non-crystalline component on the basis of the sharpness in terms of ΔQ and as a consequence, the orientation parameters for each component can be obtained [24]. Table 2 shows the values of $\langle P_2 \rangle_x$ for the crystalline component together with a measure of the crystalline scattering associated with the total scattering at the point of the (110) peak. Whilst the fraction of crystalline scattering can be seen to be approximately equal for all three PEs, $\langle P_2 \rangle_x$ varies significantly from sample A to C. In summary, all three systems exhibit global anisotropy when crystallized from a melt with a previous shear rate $> \dot{\gamma}_c$. However, some variation in both the crystal texture and level of preferred orientation is observed. In particular, $\langle P_2 \rangle_x$ does not depend in any simple way on the fraction of highest molecular weight. The highest $\langle P_2 \rangle_x$ value was obtained from the sample with the lowest M_w and M_n values and the intermediate ultra-high molecular weight composition.

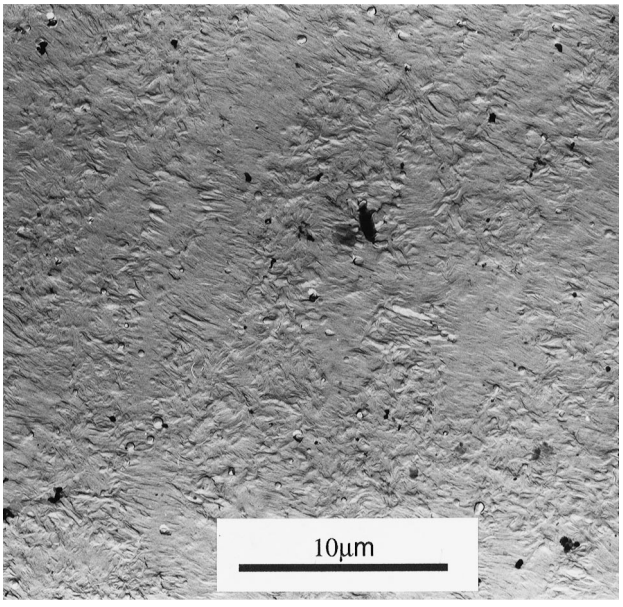

Fig. 7. TEM micrograph of PE sample A, crystallized at 120°C from a melt at 140°C sheared at 40 s^{-1}.

3.2. Morphology

Figs. 7–9 display TEM micrographs from the melt sheared and crystallized PE samples A–C respectively. Fig. 7 displays the morphology of sample A, the sample containing the largest proportion of ultra-high molecular weight material (i.e. exhibits the highest τ_{250}) and reveals shish kebabs with the cores oriented about a common axis with overgrowth lamellae orthogonal to the row nuclei. This axis again lies at $\sim 20°$ to the direction of shear, in line with the X-ray data (Fig. 3). This figure indicates that the row nucleated structures are each ~ 3 μm wide and closely packed together. Fig. 8 displays the morphology seen in material B, the sample containing the lowest proportion of high molecular weight material, which is markedly different from sample A. No shish kebabs are evident: rather the micrograph reveals an apparently unoriented lamellar morphology. This observation is qualitatively surprising, in that WAXS reveals evidence of extensive global orientation. In fact, from Figs 4 and 5 and from Table 2, it is evident that at a molecular level, this system is more highly oriented than the classic shish-kebab texture that can be seen in Fig. 7. Fig. 9 reveals the morphology of sample C: shish kebabs of similar dimensions to those seen in sample A are evident, and are packed equally closely. It is clear from the figure, however, that these row nuclei exist in specific domains, whilst other areas of the sample are apparently devoid of any preferential orientation. It is clear that material C has molecular characteristics intermediate to those for materials A and B, both in terms of its ultra-high molecular weight content (Table 1) and in the resultant crystalline orientation (Table 2). The first peak in the molecular weight distribution is closer to the principal peak in B, while the second peak for C is closer to the main peak for A. However, the morphology is only intermediate in the sense that it is a spatially separated linear combination of the two characteristic microstructures described above. Thus, whilst it would appear that the extent of molecular orientation, at a segmental level that can develop during crystallization from sheared melts can vary continuously, the lamellar texture switches abruptly from lamellar to shish-kebab. This variation is in response to local conditions within the melt and an explanation for this unexpected discontinuous behaviour is proposed below.

4. Discussion

We feel that the results presented above reveal important facts about the nature of the development of oriented structures from melt sheared samples of linear polyethylene. Whilst the results confirm simple notions regarding shish kebabs, they also provide new insights into the subtle processes that influence the formation of crystalline structure from a deformed melt in PE. It is self-evident that these results have direct relevance to film blowing and blow

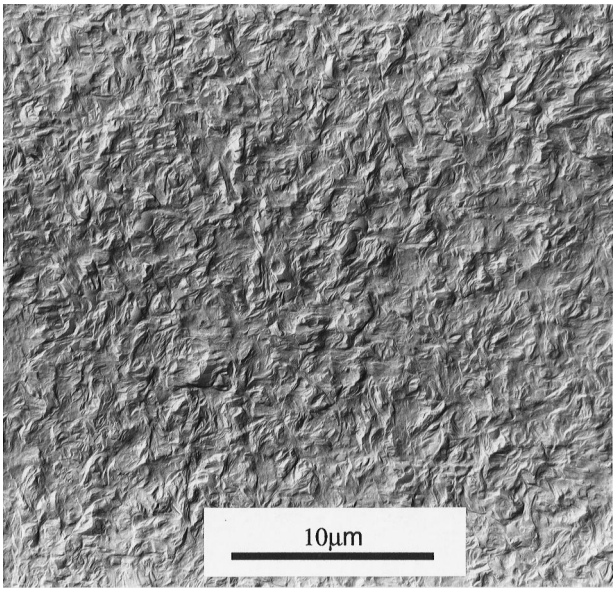

Fig. 8. TEM micrograph of PE sample B, crystallized at 120°C from a melt at 140°C sheared at 40 s^{-1}.

moulding and other low orientation polymer processing procedures rather than the spinning of highly oriented fibres.

It is clear that the critical shear rate $\dot{\gamma}_c \sim 1\ s^{-1}$ is not related simply to the subsequent formation of shish kebabs. Material B, which does not have a significant ultra-high molecular weight tail, forms a macroscopically oriented crystalline morphology without the development of a shish kebab texture. Since the other two materials both contain an equivalent upper molecular weight fraction as B, the formation of shish kebabs must be over and above such effects. It is reasonable to expect that the critical shear rate for shish kebab formation, if it were possible to identify, would exhibit considerable variation. Nevertheless it is clear that the critical shear rate for the development of a globally oriented crystal texture remains at the same order of magnitude for all of the three molecular weight distributions investigated here.

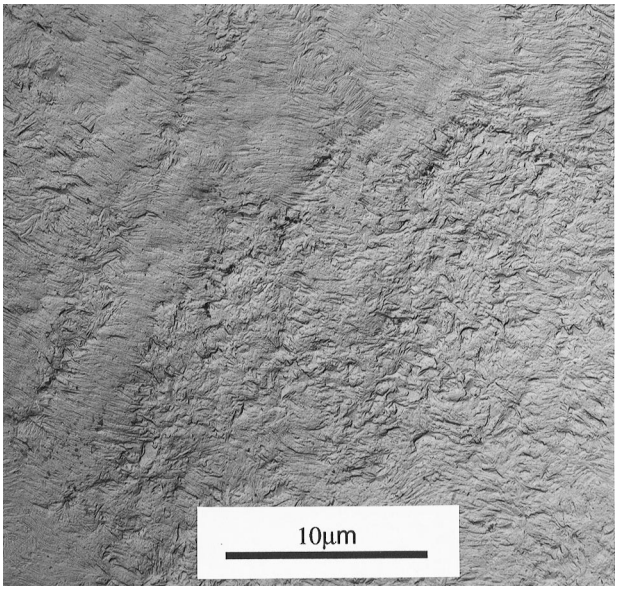

Fig. 9. TEM micrograph of PE sample C, crystallized at 120°C from a melt at 140°C sheared at 40 s^{-1}.

The observation of row nucleated structures in the morphology of sample A confirms existing expectation: they suggest that the longest molecules are extended to a high degree in the deformed melt, and thus, by reason of their associated longer relaxation times, remain extended as the sample crystallizes. These extended chains then bear the majority of the stress imposed on the network, with the shorter molecules forming chain folded lamellar overgrowth upon the central core. Results obtained from material A are therefore in good agreement with existing literature (see, for example, Refs. [1–8]). Considered in isolation, the absence of shish kebabs in sample B is then explained by the reduced high molecular weight tail in this sample. However, this neglects the global orientation revealed by WAXS which, in sample B, significantly exceeds that in sample A despite its apparently unoriented lamellar texture. Taken together, these results emphasize both the role of various molecular weight fractions and the way in which these interact with each other in the realization of these strikingly different morphologies.

The value of combining the techniques of WAXS and TEM to analyze these effects is particularly evident in the results displayed in Figs 7 and 8. The WAXS azimuthal profile of Fig. 5 clearly describes a structure of greater overall orientation than those observed in Figs 4 and 5, yet the morphology of sample B exhibits no discernible macroscopic orientation. Furthermore, the analysis reveals that sample C, which has the intermediate proportion of high molecular weight material, describes an intermediate condition only in the global case: it locally contains elements of each extreme case in discrete domains. The shish kebabs contained within sample C are of the same longitudinal and transverse dimensions as those in sample A, and the region free of such structures (towards the right in Fig. 9) is apparently as isotropic as sample B. This observation has important implications. Since it would seem unlikely that extensive spatial variations in molecular composition exist on this scale within the melt, the transition between the non-shish kebab state and the proliferation of shish kebabs must be considered in terms of a local density of different nucleation sites, rather than any specific global conditions. Thus, Fig. 9 is accounted for in terms of a region where an insufficiency of linearly extended molecules leads to no apparent macroscopic orientation of any form whereas, in a different region, the density of extended arrays of row nuclei is such that shish kebabs become the preferred morphological form. Significantly, these have the same dimensions and the same orthogonal lamellar overgrowth as those seen in the high molecular weight PE grade A. This result is in good agreement with a recent investigation by coworkers into the crystallization of sheared PE, which indicates that the

dimensions of the shish kebabs are determined by the crystallization temperature, and the angle subtended by the epitaxial lamellae at the core is a function of the applied shear rate [25].

Whether the shish kebab texture dominates over the apparently isotropic morphology will depend on the relative nucleation and growth rates of each characteristic texture as well as the relative populations of the associated nuclei. The shish kebab texture depends on the presence of extensive continuity of oriented nuclei. Where the length of the linear nucleating core greatly exceeds the width of the associated chain-folded lamellae, the resultant structural features appear as classic shish kebabs, where this criterion is not met, sheaf-like structures will develop. Nevertheless, the mechanism of nucleation in these two cases is, we suggest, fundamentally equivalent, despite the apparently different morphologies that result. The role of extended molecular conformations in the early stages of spherulitic growth has been demonstrated in isotactic polystyrene, where stacks of one to 10 lamellar crystals connected by an extended molecular core have been observed [26]. Thus, the morphology shown in Fig. 8 is most reasonably explained in terms of profuse nucleation through an identical mechanism; small elongated nuclei are formed as a result of the extension of molecular segments in response to local flow fields. However, as a result of their limited extent combined with misalignment about the macroscopic axis of shear flow, the morphology appears lamellar in nature.

5. Conclusions

These results demonstrate graphically both the subtle nature of crystallization from a sheared melt and also the dramatic structural changes that can be induced by small changes in the molecular weight distribution. We have demonstrated the co-operative nature of crystallization and shown how two different textures (shish kebabs and apparently unoriented lamellar) can both form systems which exhibit high levels of preferred molecular orientation.

In particular, the results emphasize that while the highest molecular weight component is important in the formation of row nucleated structures from a deformed PE melt, very different morphologies arise, after identical shear and crystallization procedures, in materials where the overall molecular weight distribution differs only slightly. We propose that the onset of the formation of a preferred orientation in the crystallized sample is dependent on a critical local density of elongated molecules which are unable to relax prior to the onset of crystallization.

At the transition, this leads to a global structure which evidences discrete domains of contrasting morphologies: shish kebabs proliferate in areas where such a critical density of contiguous nuclei is exceeded, and are not seen in domains which do not possess sufficiently extended linear core structures. Whereas a ultra-high molecular weight tail is required to develop the shish kebab structure, the presence of more modest molecular weight material when subjected to shear rates above $\dot{\gamma}_c$ will lead to a macroscopically oriented system with similar or higher levels of preferred orientation.

Acknowledgements

This work is supported by the EPSRC through GR/J99025 and a CASE award for JAP with BP Chemicals. SJS acknowledges financial support from the Royal Society, under the Royal Society Return Fellowship programme.

References

[1] Peterlin A. Pure Appl Chem: Macromol Chem 1973;8:277.
[2] Peterlin A. In: Miller RL, editor. Flow-induced crystallization in polymer systems, Midland Macromolecular Monographs, Vol. 6, Chapter 1. New York: Gordon and Breach Science Publishers, 1979.
[3] Keller A, Machin MJ. J Macromol Sci Phys Ed (B) 1967;1:41.
[4] Hay JN, Keller A. J Materials Sci 1967;2:538.
[5] Ulrich RD, Price FP. J Appl Polym Sci 1976;20:1077.
[6] Hsiue ES, Robertson RE, Yeh GSY. Polym Eng and Sci 1983;23:74.
[7] Bashir Z, Odell JA, Keller A. J Mater Sci 1984;19:3713.
[8] Bashir Z, Odell JA, Keller A. J Mater Sci 1986;21:3993.
[9] Eder G, Janeschitz-Kriegl H, Liedauer S, Schausberger A, Stadlbauer W, Schindlauer G. J Rheol 1989;33:805.
[10] Eder G, Janeschitz-Kriegl H, Liedauer S. Prog Polym Sci 1990;15:629.
[11] Liedauer S, Eder G, Janeschitz-Kriegl H. Intern Polym Proc X 1995;3:243.
[12] Monasse B. J Mater Sci 1995;30:5002.
[13] Tribout C, Monasse B, Haudin JM. Colloid Polym Sci 1996;274:197.
[14] Pople JA, Mitchell GR, Chai CK. Polymer 1996;37:4187.
[15] Ferry JD. Viscoelastic properties of polymers, 3rd ed. New York: Wiley, 1980.
[16] Chai CK, Dixon NM, Gerrard DL, Reed W. Polymer 1995;36:661.
[17] Pople JA, Mitchell GR, Chai CK. Adv in X-ray Analysis 1995;38:531.
[18] Pople JA, Keates PA, Mitchell GR. J Synch Rad 1997;4:267–278.
[19] Mitchell GR. In: Booth C, Price C, editors. Comprehensive polymer science, Vol. I, Chapter 31. New York: Pergamon Press, 1989.
[20] Lovell R, Mitchell GR. Acta Cryst 1981;A37:135.
[21] Olley RH, Hodge AM, Bassett DC. J Polym Sci, Polym Phys Ed 1979;17:627.
[22] Vaughan AS. Sci Prog Oxford 1992;76:1.
[23] Olley RH, Bassett DC. Polymer 1982;23:1797.
[24] Mitchell GR. Polymer 1984;25:1562–1572.
[25] Hosier IL, Bassett DC, Moneva IT. Polymer 1995;36:4197.
[26] Vaughan AS, Bassett DC. Polymer 1988;29:1397.